

## Defect-Unbinding and the Bose-Glass Transition in Layered Superconductors

C. J. van der Beek,<sup>1</sup> M. Konczykowski,<sup>1</sup> A. V. Samoilov,<sup>2</sup> N. Chikumoto,<sup>3</sup> S. Bouffard,<sup>4</sup> and M. V. Feigel'man<sup>5</sup>

<sup>1</sup>Laboratoire des Solides Irradiés, CNRS 7642 & CEA/DSM/DRECAM, Ecole Polytechnique, 91128 Palaiseau, France

<sup>2</sup>Applied Materials, Inc., 3050 Bowers Avenue, M/S 0115, Santa Clara, California 95054

<sup>3</sup>Superconductivity Research Laboratory, ISTEK, Minato-ku, Tokyo 105, Japan

<sup>4</sup>Centre Interdisciplinaire de Recherche Ions Lasers (C.I.R.I.L.), B.P. 5133, 14040 Caen Cedex, France

<sup>5</sup>Landau Institute of Theoretical Physics, Moscow, Russia

(Received 17 March 2000)

The low-field Bose-glass transition temperature in heavy-ion irradiated  $\text{Bi}_2\text{Sr}_2\text{CaCu}_2\text{O}_{8+\delta}$  increases progressively with increasing density  $n_d$  of irradiation-induced columnar defects, but saturates for  $n_d \geq 1.5 \times 10^9 \text{ cm}^{-2}$ . The maximum Bose-glass temperature corresponds to that above which diffusion of two-dimensional pancake vortices between vortex lines becomes possible, and the “linelike” character of vortices is lost. We develop a description of the Bose-glass line that quantitatively describes experiments on crystals with widely different track densities and material parameters.

DOI: 10.1103/PhysRevLett.86.5136

PACS numbers: 74.60.Ec, 74.60.Jg, 74.60.Ge

Heavy-ion irradiated (HII) layered superconductors [1,2] have recently drawn attention, because the irradiation-induced amorphous columnar tracks help overcome the detrimental effects of high material anisotropy [3–7], and partially re-establish long-range superconducting phase order [8]. Heavy-ion irradiation increases the irreversibility field  $B_{\text{irr}}(T)$ , below which the  $I(V)$  curve is nonlinear due to vortex pinning on the tracks [9], to values well above the field  $B_{\text{FO}}(T)$  at which the first order vortex lattice-to-liquid transition field takes place in the pristine material [10]. At inductions  $B_{\text{FO}}(T) \ll B \ll B_{\text{irr}}(T)$ , the irradiated superconductor displays the phenomenology of the Bose-glass phase of localized vortices [4,9,11]; moreover, the transport properties show a distinct anisotropy related to the presence of the tracks [3–6] that is absent in the pristine material [7], and which suggests that the vortices behave as well-defined separate lines, i.e., in the Bose-glass vortex lines are disentangled.

The  $B_{\text{irr}}(T)$  line and the occurrence of flux-line entanglement are intimately related in moderately anisotropic HII superconductors such as  $\text{YBa}_2\text{Cu}_3\text{O}_{7-\delta}$  [12]. There,  $B_{\text{irr}}(T) \sim B_{\text{BG}}(T)$  corresponds to the second order phase transition line between the Bose glass and the vortex liquid [11–13];  $B_{\text{BG}}(T)$  increases with increasing columnar defect density  $n_d$ , to an upper limit attained when  $n_d \approx 1 \times 10^{11} \text{ cm}^{-2}$  (corresponding to a “matching” field  $B_\phi \equiv \Phi_0 n_d = 2 \text{ T}$ ). Departing from the correspondence of vortex lines with interacting-boson world lines in two dimensions (2D) [11,14], it was argued [12] that the upper limit of  $B_{\text{BG}}(T, n_d)$  corresponds to the field beyond which the (entangled) vortex liquid becomes stable with respect to the introduction of linear defects. In  $\text{YBa}_2\text{Cu}_3\text{O}_{7-\delta}$ , these produce a rather weak pinning near  $B_{\text{BG}}(T)$ , due to inter-vortex repulsion [15,16] and the averaging effect of vortex thermal excursions [14,17].

The situation in layered superconductors such as  $\text{Bi}_2\text{Sr}_2\text{CaCu}_2\text{O}_{8+\delta}$  is *a priori* different. First, the weak coupling between adjacent  $\text{CuO}_2$  bilayers (with separation

$s \approx 1.5 \text{ nm}$ ) implies that vortex lines are extremely soft. Over the larger part of the first Brillouin zone of the vortex lattice, the contribution of the dipole interaction between “pancake” vortices in adjacent bilayers to the tilt modulus  $c_{44}$  is expected to exceed that of the line tension  $\varepsilon_1$ , which is determined by the interlayer Josephson coupling [18,19]. Flux lines are then better described as stacks of pancakes and the analogy with the 2D boson system is no longer valid [20]. As a consequence, pinning near  $B_{\text{irr}}(T)$  in HII  $\text{Bi}_2\text{Sr}_2\text{CaCu}_2\text{O}_{8+\delta}$  is not weak: at fields  $B \lesssim \frac{1}{6} B_\phi$  pancake vortices gain maximum free energy by remaining localized on the columnar defects, even in the vortex liquid phase [21]. Nevertheless, a well-defined transition from slow nonlinear vortex dynamics in the Bose glass [4,9] to Ohmic response in the vortex liquid [5,6] does exist near the irreversibility line in  $\text{Bi}_2\text{Sr}_2\text{CaCu}_2\text{O}_{8+\delta}$ .

In order to cast light on the mechanism of this transition, we have measured  $B_{\text{irr}}(T)$  in HII  $\text{Bi}_2\text{Sr}_2\text{CaCu}_2\text{O}_{8+\delta}$  for widely varying track density and oxygen content. The latter determines the values of the anisotropy parameter  $\gamma$  and the penetration depth  $\lambda_{ab}(T)$  [22]: both increase as one decreases the oxygen content towards optimal doping. It turns out that the phenomenological behavior of  $B_{\text{irr}}(T)$  at low fields is rather similar to that found in  $\text{YBa}_2\text{Cu}_3\text{O}_{7-\delta}$ .  $B_{\text{irr}}(T)$  increases progressively towards higher values with increasing defect density, but saturates for  $n_d \geq 1.5 \times 10^9 \text{ cm}^{-2}$ , or  $B_\phi \geq 30 \text{ mT}$ . For higher matching fields, the low-field portion ( $B \lesssim \frac{1}{6} B_\phi$ ) of  $B_{\text{irr}}(T)$  adopts a strictly exponential temperature dependence. Although  $T_{\text{irr}}(B)/T_c$  strongly increases when the value of  $\lambda_{ab}$  decreases, we shall see that this increase is not due to the increase of the pinning energy.

$\text{Bi}_2\text{Sr}_2\text{CaCu}_2\text{O}_8$  crystals were grown at the University of Tokyo using the traveling-solvent floating-zone method, and postannealed at either 800 or 500 °C. This produces  $T_c$ 's of 89 K (optimal doping) and 82 K (overdoped), respectively [22]. The crystals were cut to rectangles of size 500 (l)  $\times$  400 (w)  $\times$  20 (t)  $\mu\text{m}^3$ , and irradiated with

varying fluences of 5.8 GeV Pb ions at GANIL in Caen, France. In every case, the ion beam was directed parallel to the sample  $c$  axis. Each ion impact created an amorphous columnar track of radius 3.5 nm traversing the sample along its entire thickness. Samples were prepared with track densities  $1 \times 10^9 \text{ cm}^{-2} < n_d < 2 \times 10^{11} \text{ cm}^{-2}$ , corresponding to  $20 \text{ mT} \leq B_\phi \leq 4 \text{ T}$ . The irradiation caused  $T_c$  to decrease:  $\partial T_c / \partial n_d = -3.6 \times 10^{11} \text{ K cm}^2$  or  $\partial T_c / \partial B_\phi = -1.8 \text{ KT}^{-1}$ . Subsequent measurements were performed using the local Hall probe ac magnetometer [4,23]. An ac field of frequency  $f$  and amplitude  $h_{ac} \sim 1 \text{ G}$ , applied parallel to the crystalline  $c$  axis, induces a periodic electric field gradient of magnitude  $\sim 2\pi\mu_0 h_{ac} f$  across the sample. Using a miniature Hall probe one measures the induction  $B_{ac}(f, T) = B'_{ac}(f, T) + iB''_{ac}(f, T)$  at the center of the sample top surface;  $B'_{ac}(f, T)$  is simply related to the screening current [23,24]. The sample is subjected to a dc field  $H_a$  (used to create the vortices) which can be rotated in a plane perpendicular to the crystalline  $ab$  plane. The rotation angle  $\Theta$  is defined such that  $\Theta \equiv 0$  for  $H_a \parallel ab$ , and  $\Theta \equiv 90^\circ$  for  $H_a \parallel c \parallel$  columnar defects.

Figure 1 shows the  $\Theta$  dependence of the fundamental and third harmonic transmittivity (defined as  $T'_H \equiv [B'_{ac}(f, T) - B'_{ac}(f, T \ll T_c)]/\mathcal{B}$  and  $|T_{H3}| \equiv |B_{ac}(3f, T)|/\mathcal{B}$  with  $\mathcal{B} \equiv B'_{ac}(f, T \gg T_c) - B'_{ac}(f, T \ll T_c)$ ) [23], measured in  $H_a = 500 \text{ G}$  on an optimally doped crystal with  $B_\phi = 2 \text{ T}$  ( $T_c = 86.2 \text{ K}$  after irradiation). While the crystal exhibits strong ac screening for  $H_a \parallel ab$  below 83.8 K, significant screening for  $H_a$  parallel to the columns starts only at 74.5 K. However, the ion-track related anisotropy of the screening current sets in at a lower temperature—here,

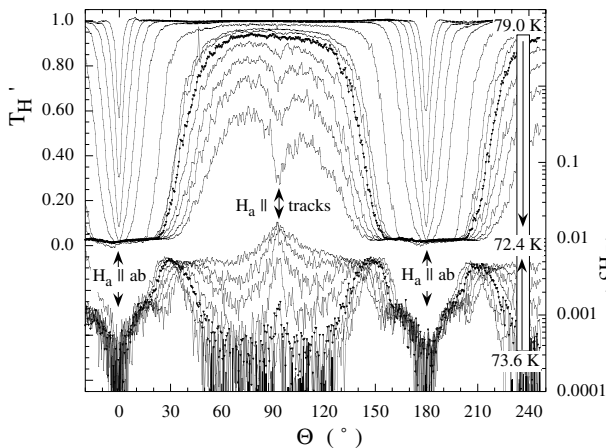


FIG. 1. Field-orientation dependence of the in-phase fundamental (upper, left-hand scale) and third harmonic (lower, right-hand scale) transmittivity for an optimally doped  $\text{Bi}_2\text{Sr}_2\text{CaCu}_2\text{O}_8$  single crystal with  $B_\phi = 2 \text{ T}$ , for temperatures from 79.0 down to 75.0 K (1 K decrement), 75.0 to 73.5 K (0.5 K decrement), and from 73.2 to 72.4 K (0.2 K decrement). The dc field  $H_a = 500 \text{ G}$ , the ac field had an amplitude of 1.5 Oe and a frequency of 44.0 Hz.

$T_{\text{irr}} \approx 73.2 \text{ K}$ . At the same temperature, a third harmonic signal first becomes discernible from the background noise for the particular orientation where the field is aligned with the ion tracks. We use the onset of a  $T_{H3}$  signal upon cooling with  $H_a$  parallel to the columns to define  $T_{\text{irr}}(B)$ , or, equivalently,  $B_{\text{irr}}(T)$ , plotted in Fig. 2. At  $B_{\text{irr}}$ , the working point enters the nonlinear part of the sample  $I(V)$  curve at an electric field of the order of  $10^{-7} \text{ Vm}^{-1}$ , corresponding to a voltage drop of  $\sim 50 \text{ pV}$  across the sample. At such low voltages, the measurement of the ac screening current may be sensitivity limited [4,24]. In practice, the use of  $h_{ac} = 1.5 \text{ Oe}$  means that the minimum measurable current density  $j_{\text{min}} \approx 5 \times 10^2 \text{ Am}^{-2}$ , comparable to a transport current of  $10 \mu\text{A}$ . The coincidence of our  $B_{\text{irr}}(T)$  with the  $B_{\text{BG}}$  data of Seow *et al.* [5] means that  $B_{\text{irr}}$  turns out to be a good approximation of the Bose-glass transition field (Fig. 2).

The evolution of  $B_{\text{irr}}(T)$  with  $B_\phi$  is plotted in Fig. 3. For  $B_\phi \leq B_\phi^{\text{min}} = 30 \text{ mT}$ ,  $B_{\text{irr}}(T)$  increases monotonically with increasing  $B_\phi$  [25]. As long as  $B_{\text{irr}}(T) < B_\phi$ , it depends exponentially on temperature, while for  $B_{\text{irr}} > B_\phi$ ,  $B_{\text{irr}} \propto (1 - T/T_c)$  [24]. For large  $B_\phi \geq B_\phi^{\text{min}}$ , one can distinguish three distinct sections of  $B_{\text{irr}}(T)$ . At all but the very lowest fields,  $B_{\text{irr}}$  again depends exponentially on  $T$ , but with the specificity that it is independent of  $B_\phi$ . In this regime [(I) in Fig. 2], there thus exists an upper limit of  $B_{\text{BG}}(T)$  in  $\text{Bi}_2\text{Sr}_2\text{CaCu}_2\text{O}_8$ , as is the case in  $\text{YBa}_2\text{Cu}_3\text{O}_{7-\delta}$  [12]. At  $B_{\text{irr}} \equiv B_{\text{int}} \sim \frac{1}{6}B_\phi$ , the exponential increase abruptly changes into a nearly vertical rise (regime II);  $B_{\text{int}}$  is the field at which intervortex repulsion starts to determine the pinned vortex configuration [21]. This transition is also manifest in the vortex liquid phase as that at which a “recoupling” transition was measured using Josephson Plasma Resonance (JPR) [8]. As  $B_{\text{irr}}$  increases to a sizable (but not constant) fraction of  $B_\phi$ , a weak temperature dependence is once again adopted,

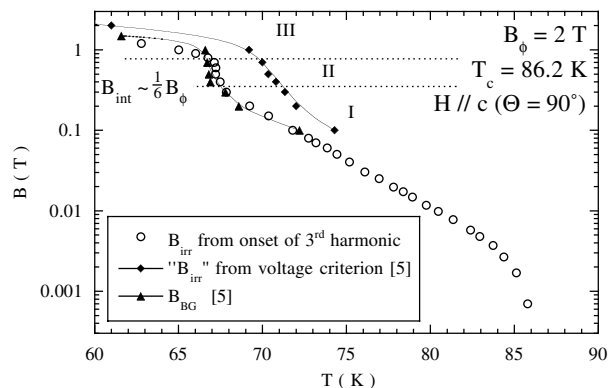


FIG. 2. The third-harmonic onset field  $B_{\text{irr}}(T)$  (O) for the same crystal as in Fig. 1. Solid symbols denote the Bose-glass transition line determined from the power-law extrapolation of the resistivity,  $\rho \propto (T - T_{\text{BG}})^s$  of a crystal with the same  $T_c$  and  $B_\phi$ , and the “irreversibility line” determined as the onset of a measurable resistivity [5].

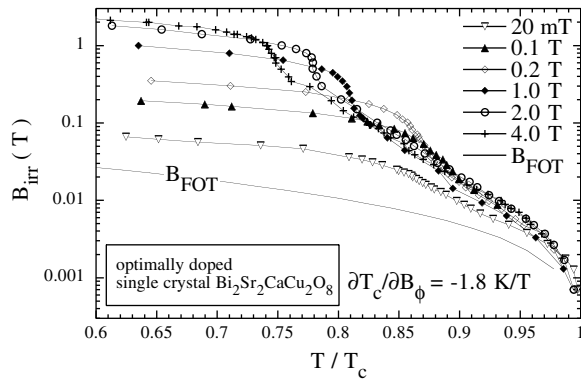


FIG. 3.  $B_{\text{irr}}(T)$  for optimally doped  $\text{Bi}_2\text{Sr}_2\text{CaCu}_2\text{O}_8$  crystals with  $B_\phi$  between 0 and 4 T. The drawn line indicates the first order phase transition  $B_{\text{FOT}}$  in a pristine crystal.

$B_{\text{irr}} \propto (1 - T/T_c)^\alpha$  with  $\alpha \gtrsim 1$  (regime III). Figure 4 shows the behavior of the irreversibility field for different oxygen content. The exponential decrease at high  $T$  is steeper for the overdoped crystal, which has the smaller  $\lambda_{ab}$  and  $\gamma$ , the larger condensation energy  $\varepsilon_0/4\pi\xi^2$ , and the stronger intervortex- and vortex-defect interaction (both are proportional to the typical vortex energy scale  $\varepsilon_0 = \Phi_0^2/4\pi\mu_0\lambda_{ab}^2$ ;  $\xi$  is the coherence length).

To describe the low-field exponential temperature dependence of  $B_{\text{irr}}(T)$ , we exploit the fact that in regime I vortex interactions are irrelevant to the column occupation [21], so that all pancakes are localized on a column. If a sufficient number of columns is available to every line (i.e., at large  $B_\phi$ ), extra free energy can be gained by the redistribution of pancakes constituting a given line over different columns. At low  $B_\phi \lesssim 0.5$  T this entropy gain is insufficient to balance the loss in vortex interaction energy, and pancakes belonging to the same line remain aligned on the same columnar defect. The superposition of the exponential portions of  $B_{\text{irr}}(T)$  for all matching fields  $30 \text{ mT} < B_\phi < 4 \text{ T}$  implies that at  $B_{\text{irr}}$  the redistribution over different column sites is irrelevant for the pancake delocalization mechanism—i.e., at and below  $B_{\text{irr}}(T)$ , pan-

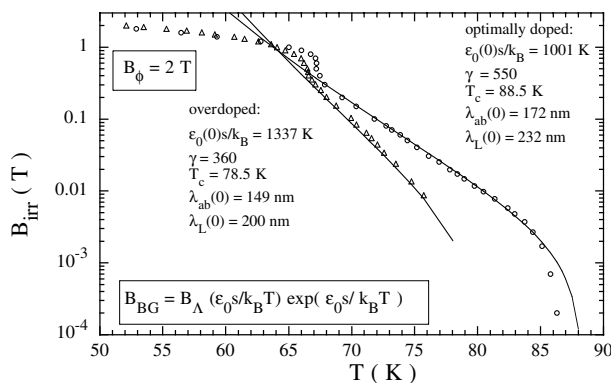


FIG. 4.  $B_{\text{irr}}(T)$  for an optimally doped ( $\circ$ ) and a lightly overdoped ( $\triangle$ )  $\text{Bi}_2\text{Sr}_2\text{CaCu}_2\text{O}_8$  crystal, both with  $B_\phi = 2$  T. Drawn lines indicate fits to Eq. (2), with parameter values as indicated.

cakes belonging to the same vortex line are well aligned on the same site, belonging to a set of allowed “columnar-defect” sites. Then, we no longer need to consider other positions in the “intercolumn space” in our model description, which becomes that of a “discrete” superconductor. Since the allowed sites are more or less equivalent, the circumstance that they are in fact columnar defect sites becomes immaterial: namely, the free energy of all vortices is lowered by approximately the same amount. The low-field vortex state therefore does not differ fundamentally from that in the *unirradiated* crystal. Only the vortex confinement in the defect potential, which plays the role of the “substrate potential” of Ref. [26], inhibits thermal line wandering and the elastic relaxation of the vortex lattice.

The main thermal excitations in this situation are expected to be small defects in the vortex lattice. In a Josephson-coupled layered superconductor, these are bound pancake vacancy-interstitial pairs within the same layer, i.e., the “quartets” of Ref. [27]. In the HII layered superconductor, such a pair corresponds to the “exchange” of one or more pancakes between two sites. The energy of the quartets is [27]

$$\varepsilon_q \approx 4c_{66}a_0^2s(R/\Lambda)^2 \approx \varepsilon_0s(R/\Lambda)^2, \quad (R \ll \Lambda), \quad (1)$$

with  $c_{66}$  the vortex lattice shear modulus,  $a_0 = (\Phi_0/B)^{1/2}$  the vortex spacing,  $R$  the distance between a bound vacancy and interstitial,  $\Lambda = [\lambda_{ab}^{-1} + (\gamma s)^{-1}]^{-1}$  the generalized penetration depth taking into account magnetic and Josephson coupling, and  $\gamma s$  the Josephson length [18,27]. In the same way as the glass transition in a layered superconductor corresponds to the pair-unbinding transition [27], the Bose glass transition is the unbinding temperature of the dislocation pairs in the “discrete” superconductor, i.e., the temperature above which pancakes can *diffuse* from line to line. We can estimate  $k_B T_{\text{BG}} = \varepsilon_q(R_l)$ , where  $R_l \approx n_l^{-1/2}$  and  $n_l$  is the equilibrium density of free dislocation pairs in the vortex liquid. Taking into account that only small pairs of size  $a_0$  (i.e., vacancies/interstitials) matter, one has  $n \approx a_0^{-2} \exp(-\varepsilon_0s/k_B T)$ ; the activation energy  $\varepsilon_0s$  is larger than that in the unirradiated superconductor because of the lack of lattice relaxation around the pair. Substituting, one has  $k_B T_{\text{BG}} = \varepsilon_0s(a_0/\Lambda)^2 \exp(\varepsilon_0s/k_B T_{\text{BG}})$ , or

$$B_{\text{BG}} = B_\Lambda \left( \frac{\varepsilon_0s}{k_B T} \right) \exp\left( \frac{\varepsilon_0s}{k_B T} \right), \quad (B_\Lambda \ll B \ll B_\phi) \quad (2)$$

with  $B_\Lambda = \Phi_0/\Lambda^2$ ,  $\varepsilon_0$ , and  $\Lambda$  to be evaluated at  $T_{\text{BG}}$ . The Bose-glass transition line does not depend on the details of the columnar defect potential such as pinning energy, column radius, or matching field. In Fig. 4, we compare Eq. (2) to the experimental results for  $\text{Bi}_2\text{Sr}_2\text{CaCu}_2\text{O}_8$  with different oxygen content. We obtain excellent *quantitative* agreement using  $\lambda_{ab}$  values from the literature [22]

and the single free parameter  $\gamma$  (contained only in  $B_\Lambda$ ). The values  $\gamma = 360$  and  $550$  found for the overdoped and the optimally doped material, respectively, are well within accepted experimental limits. The deviations near  $T_c$  are possibly due to surface barrier effects [24]. Thus, Eq. (2) reproduces the correct field, temperature,  $B_\phi$ , and doping dependence of the Bose-glass line.

The Bose-glass transition separates the low- $T$  phase in which pancake vortices can wander between columnar defects, but always remain bound to the same site, or vortex line, from the high  $T$  phase in which diffusion of pancakes between sites (lines) is possible. Below  $T_{BG}$ , individual pancakes (“defect pairs”) cannot provide flux transport at low currents; vortex lines can only move as a whole, leading to the linelike behavior observed in Refs. [3–7]. Oppositely, the pancake diffusion above  $T_{BG}$  not only implies an Ohmic resistivity [5,6], but also that the linear nature of the vortex lines no longer appears in the angular dependence of the transport properties. This is exactly what is observed in Fig. 1. The intersite diffusion of pancakes (or “pancake exchange”) means that at  $T > T_{BG}$  vortex lines are effectively entangled, on a scale  $l = s \exp(\epsilon_0 s / k_B T)$ . The upper limit of the Bose-glass transition in layered superconductors is thus analogous to that in moderately anisotropic compounds in that it represents the boundary at which vortices become delocalized into an entangled flux liquid.

The meaning of  $B_\Lambda$  becomes apparent from Eq. (1), where  $\Lambda$  appears as the typical interaction distance between small dislocation pairs. For separations  $\gg \Lambda$ , i.e., for matching fields  $B_\phi \ll B_\Lambda$ , the formation of quartets demands a (shear) energy cost that is much greater than either  $\epsilon_0 s$  or  $k_B T$ . The excitation of a pancake onto another site is then unlikely even in the vortex liquid. Delocalization will occur as it does in a moderately anisotropic superconductor: thermal wandering of the vortices into the intercolumn space lowers their binding energy until they can be liberated from the columns by thermal activation [4]. Similarly, in regime II ( $B > \frac{1}{6} B_\phi$ ), where the number of available tracks is insufficient not because of the intercolumn distance but because of track occupation by other vortices, delocalization is initiated by pancake wandering into the intercolumn space. Then,  $B_{irr}(T)$  increases with decreasing  $B_\phi$  because the number of available sites decreases. The experimentally found condition  $B < \frac{1}{6} B_\phi$  on the validity of Eq. (2) also describes its validity range at low  $B_\phi$ :  $B_{irr}$  becomes ion-dose dependent when  $B_\phi < B_\phi^{\min} = 6B_\Lambda$ , in excellent agreement with the experimental values  $B_\phi^{\min} \sim 30$  mT and  $B_\Lambda = 7.0$  mT (4.5 mT) found for overdoped (optimally doped)  $\text{Bi}_2\text{Sr}_2\text{CaCu}_2\text{O}_8$ , respectively.

Summarizing, in the regime of individual vortex line pinning by columnar defects in a layered superconductor, the upper limit of the Bose-glass transition corresponds

to the onset of pancake vortex diffusion between different lines and flux-line entanglement. However, in both the glass and the vortex liquid phases, *only* columnar defect sites are available to the pancakes; hence, a modelization in terms of a “discrete superconductor” is appropriate. The onset of diffusion in this discrete superconductor presents a realization of the glass transition by unbinding of small defect pairs proposed in Ref. [27]; in the original continuous problem of an unirradiated layered superconductor, the defect-unbinding mechanism is masked by strong Gaussian thermal fluctuations [18].

We thank V. B. Geshkenbein, P. H. Kes, A. E. Koshelev, P. LeDoussal, and V. M. Vinokur for stimulating discussions. This work was supported by the E.S.F. “VORTEX” program and a NATO grant for International Collaboration in Research; M. V. F. was supported by DGA Grant No. 94-1189.

- 
- [1] V. Hardy *et al.*, *Physica* (Amsterdam) **205C**, 371 (1993).
  - [2] M. Konczykowski *et al.*, *J. Alloys Compd.* **195**, 407 (1993).
  - [3] L. Klein *et al.*, *Phys. Rev. B* **48**, 3523 (1993).
  - [4] C. J. van der Beek *et al.*, *Phys. Rev. Lett.* **74**, 1214 (1995).
  - [5] W. S. Seow *et al.*, *Phys. Rev. B* **53**, 14 611 (1996).
  - [6] R. Doyle *et al.*, *Phys. Rev. Lett.* **77**, 1155 (1996).
  - [7] D. Zech *et al.*, *Phys. Rev. B* **52**, 6913 (1995).
  - [8] M. Sato *et al.*, *Phys. Rev. Lett.* **79**, 3759 (1997); M. Kosugi *et al.*, *Phys. Rev. Lett.* **79**, 3763 (1997); M. Kosugi *et al.*, *Phys. Rev. B* **59**, 8970 (1999).
  - [9] M. Konczykowski *et al.*, *Phys. Rev. B* **51**, 3957 (1995).
  - [10] E. Zeldov *et al.*, *Nature* (London) **375**, 373 (1995).
  - [11] D. R. Nelson and V. M. Vinokur, *Phys. Rev. Lett.* **68**, 2398 (1992); *Phys. Rev. B* **48**, 13 060 (1993).
  - [12] A. V. Samoilov *et al.*, *Phys. Rev. Lett.* **76**, 2798 (1996).
  - [13] W. Jiang *et al.*, *Phys. Rev. Lett.* **72**, 550 (1994).
  - [14] J. Blatter *et al.*, *Rev. Mod. Phys.* **66**, 1125 (1994).
  - [15] A. V. Samoilov and M. Konczykowski, *Phys. Rev. Lett.* **75**, 186 (1995).
  - [16] C. Wengel and U. C. Täuber, *Phys. Rev. Lett.* **78**, 4845 (1997); *Phys. Rev. B* **58**, 6565 (1998).
  - [17] M. V. Feigel'man and V. M. Vinokur, *Phys. Rev. B* **41**, 8986 (1990).
  - [18] L. Glazman and A. E. Koshelev, *Phys. Rev. B* **43**, 2835 (1991).
  - [19] G. Blatter *et al.*, *Phys. Rev. B* **54**, 72 (1996).
  - [20] A. E. Koshelev, P. Le Doussal, and V. M. Vinokur, *Phys. Rev. B* **53**, R8855 (1996).
  - [21] C. J. van der Beek *et al.*, *Phys. Rev. B* **61**, 4259 (2000).
  - [22] T. W. Li *et al.*, *Physica* (Amsterdam) **257C**, 179 (1996).
  - [23] J. Gilchrist and M. Konczykowski, *Physica* (Amsterdam) **212C**, 43 (1993).
  - [24] C. J. van der Beek *et al.*, *Phys. Rev. B* **51**, 15 492 (1995).
  - [25] B. Khaykovich *et al.*, *Phys. Rev. B* **57**, R14 088 (1998).
  - [26] M. J. W. Dodgson, V. B. Geshkenbein, and G. Blatter, *Phys. Rev. Lett.* **83**, 5358 (1999).
  - [27] M. V. Feigel'man, V. B. Geshkenbein, and A. I. Larkin, *Physica* (Amsterdam) **167C**, 117 (1990).